Synthesis and Characterization of Fully Aliphatic Polyimides from an Aliphatic Dianhydride with Piperazine Spacer for Enhanced Solubility, Transparency, and Low Dielectric Constant

Pradip Kumar Tapaswi, Myeon-Cheon Choi, Young Sik Jung, Hun Jeong Cho, Deok Jin Seo, Chang-Sik Ha

Department of Polymer Science and Engineering, Pusan National University, Busan 609–735, Republic of Korea
Correspondence to: C.-S. Ha (E-mail: csha@pnu.edu)

Received 27 March 2014; accepted 3 May 2014; published online 20 May 2014
DOI: 10.1002/pola.27242

ABSTRACT: A new series of fully aliphatic polyimide (API) based on a novel aliphatic dianhydride monomer-2,2′-(1,4-piperazinediyl)-disuccinic anhydride (PDA), in which two units of succinic anhydride have been connected by an aliphatic heterocyclic piperazine spacer that possesses aminomethylene (-NCH_2) moiety in the aliphatic/alicylic backbone capable of inducing charge transfer (CT) interactions in the polyimide network, was successfully synthesized. The APIs were soluble in common polar organic solvents. The polyimide films of PDA with alicyclic diamines were almost colorless. T_{10} (temperature of 10% weight loss) of APIs were ranged from 299–418 °C and T_g of API3-API6 were in the temperature range of 170 to 237 °C. The light-colored polyimide films of API3-API6 possessed good mechanical properties with tensile strength of 54–72 Mpa, tensile modulus of 1.6–2.3 Gpa and elongation at break of 4–9%. The polyimide films of API3-API6 were highly flexible and free-standing which is quite rare in fully APIs. The dielectric constant of one of the synthesized API (API4) was as low as 2.14. © 2014 Wiley Periodicals, Inc. J. Polym. Sci., Part A: Polym. Chem. **2014**, *52*, 2316–2328

KEYWORDS: aliphatic polyimides; dielectric properties; piperazine spacer; free-standing polyimide film; good mechanical properties; high-temperature materials; low dielectric constant; polyimides; transparency

INTRODUCTION Polyimides, a class of high-performance macromolecules characterized by outstanding thermal stability, mechanical, electrical, and solvent resistance properties originating from their rigid backbones, often find extensive applications in photoresists, passivation and dielectric films, soft print circuit boards, and alignment films within displays.[1,2] The main obstacles that seriously limit the applications of aromatic polyimides in optoelectric materials and high-speed multilayer printed wiring boards are their insolubility in common organic solvents in the fully imidized form, the light or dark-yellow color of their films caused by intra- and intermolecular charge transfer (CT) interactions, and their high dielectric constants.[3–5.]

In recent years, polyimides with high optical transparencies and low dielectric constants have been in demand for optoelectronic and microelectronic applications. Alicyclic and aliphatic polyimides (APIs) are candidates for applications in optoelectronics and interlayer dielectrics due to their higher transparency and low dielectric constants when compared to aromatic polyimides.[6–13] These properties result from their low molecular density, low polarity, and low probability of undergoing inter- or intramolecular charge transfer.[14] Accordingly, great effort has been made to synthesize new aliphatic/alicyclic dianhydride or diamine monomers. Schenk et al. reported the synthesis of *cis*-cyclobutane-l,2,3,4-tetracarboxylic dianhydride by irradiating a solution of maleic anhydride in dioxane with a high-pressure mercury lamp.[15] Suzuki et al. synthesized a substituted 1,2,3,4-cyclobutanetetracarboxylic dianhydride by photodimerization of maleic anhydrides.[16] The 1,2,4-tricarboxyl-3-methylcarboxyl cyclopentane dianhydride was obtained by oxidizing a Diels–Alder adduct of cyclopentadiene and maleic anhydride with nitric acid, followed by neutralization and subsequent dehydration.[17–19] The procedure for the synthesis of 1,3-diaminoadamantane was first reported by Smith et al. and was later modified by Chern *et al.*[20,21] Polyimides synthesized from these monomers showed excellent transparency and good solubility and moderate to good thermal properties. However, in most of the cases, the mechanical properties of fully alicyclic/API films were not good as the films were too much brittle.[22] Recently, Bin et al. reported that trimethyleneamino

Additional Supporting Information may be found in the online version of this article.

(-$(CH_2)_3$N) group can induce significant CT interaction even in fully API network that could lead to the synthesis of high modulus API.[23] Therefore, incorporating rigid alicyclic structures with some electron donor/acceptor atoms or group that can induce some sort of moderate to weak CT interaction in the polymer network, may lead to the synthesis of transparent, soluble aliphatic/alicyclic polyimides with good thermal and mechanical properties. We were driven by this fact in designing the aliphatic dianhydride monomer. Here, we report the successful synthesis of novel fully APIs based on a novel aliphatic dianhydride monomer-2,2′-(1,4-piperazinediyl)-disuccinic anhydride (PDA), in which two units of succinic anhydride have been connected by an aliphatic heterocyclic piperazine spacer that possesses aminomethylene (-NCH_2) moiety in the aliphatic/alicylic backbone capable of inducing CT interactions in the polyimide network. The optical, dielectric, thermal, physical, and mechanical properties of those polymers were also thoroughly investigated and are discussed in this paper.

EXPERIMENTAL

Materials

The alicyclic diamine, 4,4′-methylene bis(2-methylcyclohexylamine) (MMCA), was distilled under reduced pressure and stored in the dark before use while 4,4'-methylene bis(cyclohexylamine) (MCA) was recrystallized from hexane and dried at 50 °C. Ethylenediamine (EN) and 1,3-diaminopropane (13DAP) were also distilled under reduced pressure before use. The solvent *m*-cresol was dried over $CaCl_2$, then over 4 Å Linde-type molecular sieves, distilled under reduced pressure, and stored under nitrogen in the dark. All other reagents and chemicals were purchased from Aldrich Chemical Company and were used as received.

Synthesis of Dimethyl Fumarate

This compound was synthesized following an already reported procedure[24] with some modifications. To fumaric acid (FA) (14.5 g, 125 mmol) suspended in MeOH (200 mL) was added concentrated H_2SO_4 (5 mL), and the mixture was heated to reflux for 1 h. The mixture was then cooled in an ice bath and neutralized with 10% Na_2CO_3 which resulted in some white precipitate to come. The precipitate was filtered and washed several times with water and finally was dried in vacuum for 12 h at 50 °C.

This compound was known and thus was characterized by melting point determination after crystallizing from hot ethylacetate (EtOAc). Yield: 91%. mp: 102 °C (EtOAc) (lit. mp 102.4 °C).

Synthesis of 2,2′-(1,4-Piperazinediyl)-di-[succinic acid]-tetramethyl ester

This compound is already reported[25] but we adapted a different synthetic procedure to simplify the synthesis. This synthesis was affected by refluxing 0.05 mol of piperazine (4.3 g) and 0.1 mol of the ester (dimethyl fumarate, DMF) (14.4 g) in 100 cc of 1,4-dioxane for 16 h. Upon cooling, the pure compound crystallizes out. The precipitate was filtered and the filtrate was concentrated and cooled to give more precipitate which was again filtered. Both of these precipitates were collected and dried in vacuum for 12 h to give a highly crystalline colorless solid.

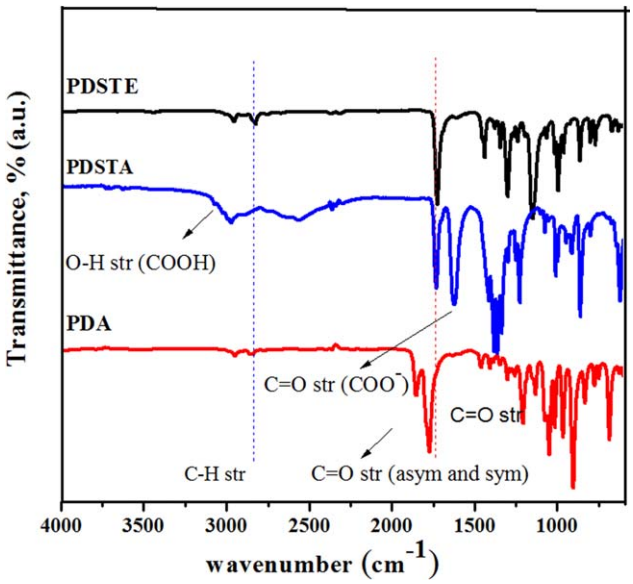

FIGURE 1 FTIR spectra of PDSTE, PDSTA, and PDA. [Color figure can be viewed in the online issue, which is available at wileyonlinelibrary.com.]

Yield: 82%. mp: 158 °C (EtOAc). ^{1}H NMR (300 MHz, $CDCl_3$, δ, ppm): 2.38–2.50 (m, 4H, Het-CH_2CH_2), 2.54–2.70 (m, 6H, β-CH_2, Het-CH_2CH_2), 2.81 (dd, $J = 16.0$ and 9.2 Hz, 2H, β-CH_2), 3.64 (s, 6H, $2OCH_3$), 3.68 (dd, 2H, overlapped signals, α-CH), 3.70 (s, 6H, $2OCH_3$) (Supporting Information Fig. S1). ^{13}C NMR (75 MHz, $CDCl_3$, δ, ppm): 171.7 and 170.9 (ester C), 63.4 (α-CH), 51.8 (OCH_3), 51.5 (OCH_3), 49.9 (Het-CH_2CH_2), 34.0 (β-CH_2) (Supporting Information Fig. S2). Anal. calcd. for $C_{16}H_{26}N_2O_8$: C, 51.33; H, 7.00; N, 7.48. Found: C, 51.19; H, 7.09; N, 7.53; FTIR (KBr, cm^{-1}): 1734 (C=O) (Fig. 1).

Synthesis of 2,2′-(1,4-Piperazinediyl)-disuccinic acid

About 0.03 mol of 2,2′-(1,4-piperazinediyl)-di-[succinic acid]-tetramethyl ester (PDSTE) (11.2 g) was taken in a 500-mL round bottomed flux containing 120 mL of 2 (N) NaOH and 120 mL of MeOH. The mixture was heated at 60 °C to dissolve the solid and was heated further for 3 h at the same temperature. Finally, the reaction mixture was cooled to room temperature which resulted in the precipitation of the tetra-acid salt. The salt was collected by filtration followed by repeated washing with MeOH. It was then dissolved in 200 mL of water and the pH of the resulting solution was adjusted carefully to 3.8 by concentrated HCl and was stirred for 0.5 h at room temperature. The precipitated white compound was filtered and washed several times with cold water. The white residue was dried in vacuum at 80 °C for overnight. 2,2′-(1,4-Piperazinediyl)-disuccinic acid (PDSTA) was not soluble in most common organic solvents as well as

in water. So, in order to make NMR sample, minimum amount of solid NaOH was used to dissolve the compound in D_2O.

Yield: 92%. mp: 218–219 °C (H_2O+MeOH). ^1H NMR (300 MHz, D_2O, δ, ppm): 2.46–2.54 (bd, 4H, Het-CH_2CH_2), 2.56–3.40 (bm, 6H, β-CH_2, Het-CH_2CH_2), 3.44–3.54 (bm, 2H, β-CH_2), 4.80 (dd, 2H, overlapped signals, α-CH) (Supporting Information Fig. S3). ^{13}C NMR (75 MHz, D_2O, δ, ppm): 178.8 ($\underline{C}OO^-$), 67.7 (α-$\underline{C}H$), 49.1 (Het-$\underline{C}H_2\underline{C}H_2$), 37.4 ($\beta$-$\underline{C}H_2$) (Supporting Information Fig. S4). Anal. calcd. for $C_{12}H_{18}N_2O_8$: C, 45.28; H, 5.70; N, 8.80. Found: C, 45.16; H, 5.79; N, 8.83. FTIR (KBr, cm^{-1}): 1723(C=O for carboxylic acid) and 1623 (C=O for carboxylate) (Fig. 1).

Synthesis of 2,2′-(1,4-Piperazinediyl)-disuccinic anhydride

PDSTA (5.4 g, 17 mmol), pyridine (8 mL), and acetic anhydride (10 mL) were placed in a 50 mL flask equipped with a condenser and a magnetic stirrer. The reaction was carried out by stirring the reaction mixture at 40 °C for 24 h in nitrogen atmosphere. The resulting anhydride after cooling at room temperature was filtered off and washed thoroughly with acetic anhydride and dry diethyl ether. The white powder was then dried under vacuum at 40 °C and recrystallized from acetic anhydride.

Yield: 60%. mp: 156 °C (decompose); ^1H NMR (300 MHz, d_6-DMSO, δ, ppm): 2.39 (bd, $J = 6.8$ Hz, 4H, Het-CH_2CH_2), 2.76 (bd, $J = 6.8$ Hz, 4H, Het-CH_2CH_2), 3.04 (d, $J = 8.4$ Hz, 4H, β-CH_2), 4.21 (t, $J = 16.4$ Hz, 2H, α-CH). ^{13}C NMR (75 MHz, d_6-DMSO, δ, ppm): 171.6 ($\underline{C}OO\underline{C}O$), 170.6 ($\underline{C}OO\underline{C}O$), 63.6 (α-$\underline{C}H$), 48.9 (Het-$\underline{C}H_2\underline{C}H_2$), 31.9 ($\beta$-$\underline{C}H_2$) (Supporting Information Fig. S5). Anal. calcd. for $C_{12}H_{14}N_2O_6$: C, 51.06; H, 5.00; N, 9.93. Found: C, 49.93; H, 5.10; N, 9.96. IR (KBr, cm^{-1}): 1860, 1781 (C=O), 1210, 1127 (C-O-C).

General Polymerization Procedure and Polyimide Film Preparation

In a 30-mL three-necked flask equipped with a mechanical stirrer were placed the dianhydride (2.0 mmol) and 4 mL of *m*-cresol. Under slow stream of nitrogen gas, the mixture was stirred until the dianhydride was entirely dissolved. Diamines (2.0 mmol) and an additional 2 mL of *m*-cresol were then added into the clear solution. The flask was heated at 60 °C, and the solution was stirred for 2 days. An aliquot of the polycondensation solution containing poly(amic acid) (PAA) was cast on a glass plate. The polyimide film was prepared by heating the glass plate at 80 °C for 3 h, at 200 °C for 1 h, and then at 250 °C for 1 h under vacuum. After curing, the glass plate was immersed in boiling water to facilitate removal of the flexible, free-standing polyimide film. API1 and API2 were too brittle and the polyimide films come off the glass surface immediately after imidization and therefore no need to immerse in water further to remove the films from the glass surface. To perform the dielectric constant and transparency measurements, the PAA solutions were spin-coated onto clean ITO glass and quartz plates, respectively, and then subjected to imidization following the heating cycle described above.

Characterization

^1H and ^{13}C NMR spectra were recorded on a Varian Unity Plus-300 (300 MHz) NMR spectrometer. Infrared spectra (KBr disks) were recorded on a Shimadzu IR Prestige-21 spm using a Ge-KBr beam splitter. Average molecular weight (M_n) and polydispersity index (PDI) of the soluble APIs were estimated by gel permeation chromatography (GPC) using a Waters 515 differential refractometer with Waters 410 HPLC Pump and two Styrogel HR 5E columns in DMF (0.1 mg L^{-1}) at 42 °C, calibrated with polystyrene standards. The solubility test was performed using equal amounts of APIs in matched quantities of commonly used solvents. The level of theory with the three-parameter Becke-style hybrid functional (B3LYP) was adopted for the density functional theory (DFT) calculations in conjunction with the Pople-type 6–311G(d,p) basis set for elucidating the molecular structures of 2,2′-(1,4-piperazinediyl)-disuccinic anhydride (PDA) and two APIs. The geometry optimization under no constraints was performed using the Gaussian-03 (Rev. D02) software installed on the TSUBAME grid cluster system in Tokyo Tech. The DFT functional and the basis set used were B3LYP/6–311++G(d,p). To investigate the thermal stability of the APIs, thermogravimetric analyses were performed under nitrogen using a TGA Q50 Q Series thermal analyzer at a heating rate of 10 °C min^{-1} from room temperature to 800 °C. Measurements of glass transition temperature were performed using a DSC Q 100 TA instrument at a heating rate of 10 °C min^{-1} under a nitrogen atmosphere. Dynamic mechanical analysis (DMA) was conducted with DMA2980 (TA instron) instrument. The storage modulus *E*, and tan δ were determined as the sample was subjected to a temperature scan mode at a programmed heating rate of 10 °C min^{-1} at a frequency of 1Hz. The transparencies of the polyimide films were measured from ultraviolet–visible spectra recorded from one accumulation on a SHIMADZU UV-1650 PC spectrometer optimized with a spectral width of 200–800 nm, a resolution of 0.5 nm, and a scanning rate of 200 nm min^{-1}; the thickness of each film was ≈15 μm. The excitation and fluorescent-emission spectra of the PI films were characterized using a Hitachi F-4500 fluorescence spectrophotometer with a resolution of 0.2 nm and a scanning rate of 240 nm min^{-1}.Wide-angle X-ray diffraction (WXAD) measurements of the pulverized samples were conducted at room temperature in the reflection mode using a Rigaku diffractometer (Model Rigaku Miniflex). The Cu Kα radiation ($\lambda = 1.54$ Å) source was operated at 50 kV and 40 mA. The 2θ scan data were collected at 0.01° intervals over the range 1.5–80° and at a scan speed of 0.58(2θ)/min. Tensile properties were determined from stress–strain curves obtained with Kyungsang Universal Testing Measurement (UTM) Materials Testing System (Model KSU.05) at a strain rate of 10 mm min^{-1} at room temperature. Measurements were performed with film specimens (50 mm in gauge length, 10 mm wide, and 0.1 mm thick). Each reported value is the average of five different measurements. The dielectric

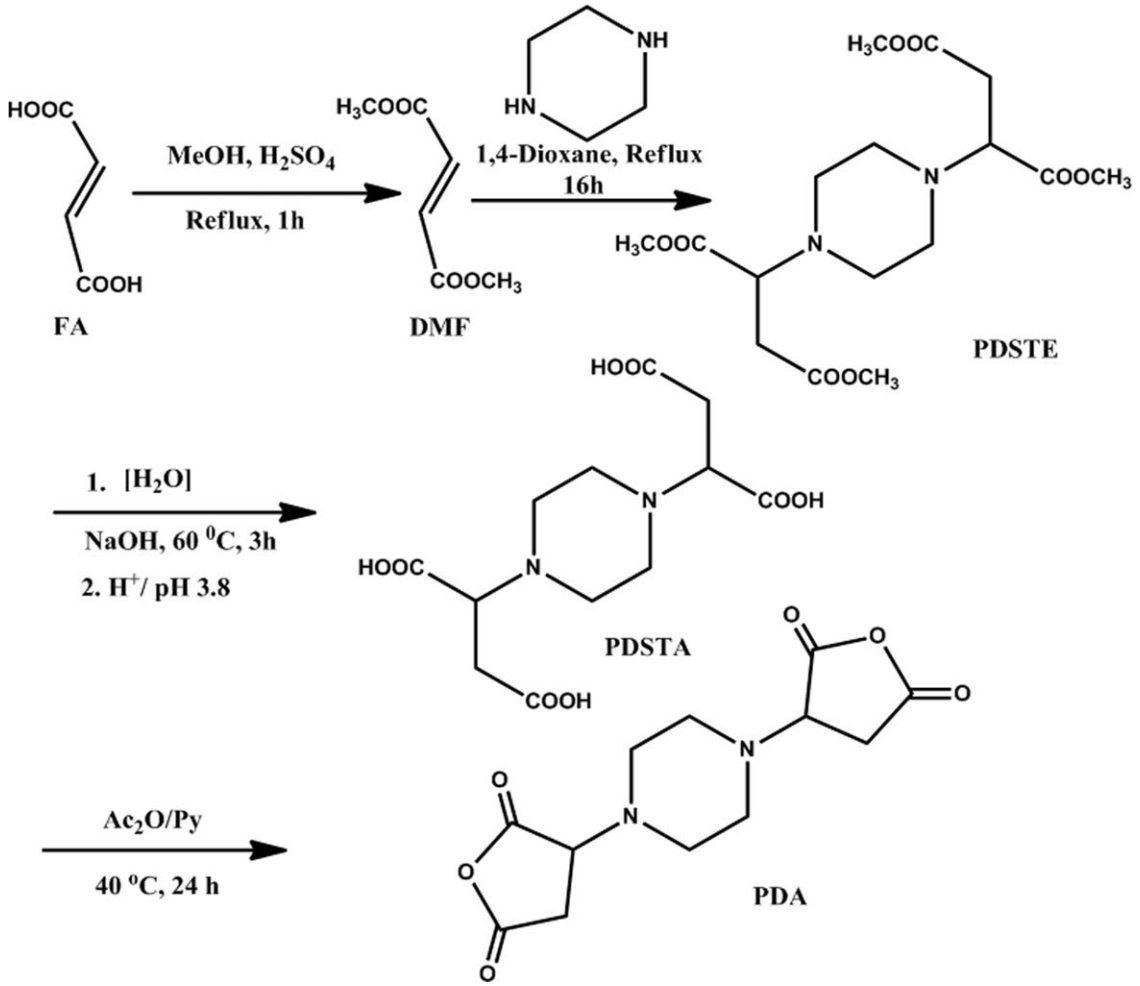

SCHEME 1 Synthesis of 2,2′-(1,4-piperazinediyl)-disuccinic anhydride (PDA).

constant (ε) was obtained at 1 MHz using an impedance-gain phase analyzer (HP4194A) and the formula $\varepsilon = C \times d/A\varepsilon_0$, where C is the observed capacitance, d is the film thickness, A is the area, and ε_0 is the free permittivity. The thickness of each film was 1.0 ± 0.05 μm. Each reported value is the average of three different measurements.

RESULTS AND DISCUSSION

Monomer Synthesis

As shown in Scheme 1, the novel piperazine containing aliphatic dianhydride monomer (PDA) was obtained through a four-step synthetic route. The first step involved the synthesis of DMF which functioned as Michael acceptor and underwent Michael addition reaction in the second step with Michael donor piperazine to yield 1,4-piperazinediyl-tetramethyldisuccinate (PDSTE). This is the key step for the synthesis of dianhydride monomer (PDA). The corresponding disuccinic acid derivative PDSTA can be obtained by the base (NaOH)-catalyzed hydrolysis of the PDSTE followed by acidification of the sodium salt of the PDSTA. Acetic anhydride in presence of pyridine had been chosen as the anhydrating agent and only after thorough optimization with various amounts of reagents, at different temperatures and reaction times it revealed that best yield can be obtained by stirring the reaction mixture at 40 °C for 24 h. At relatively higher temperatures, a black pasty mass appeared which made the purification of the dianhydride extremely difficult. The optimized condition for the synthesis of novel piperazine containing dianhydride monomer was to stir the reaction mixture at 40 °C for 24 h at N_2 atmosphere. The detailed characterizations on the dianhydride monomer (PDA) were done by FTIR (Fig. 1), ^{1}H NMR (Fig. 2), ^{13}C NMR (Supporting Information Fig. S5) spectroscopy, and elemental analyses,

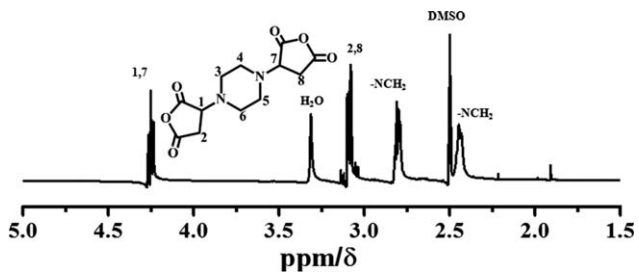

FIGURE 2 ^{1}H NMR spectrum of PDA in d_6-DMSO.

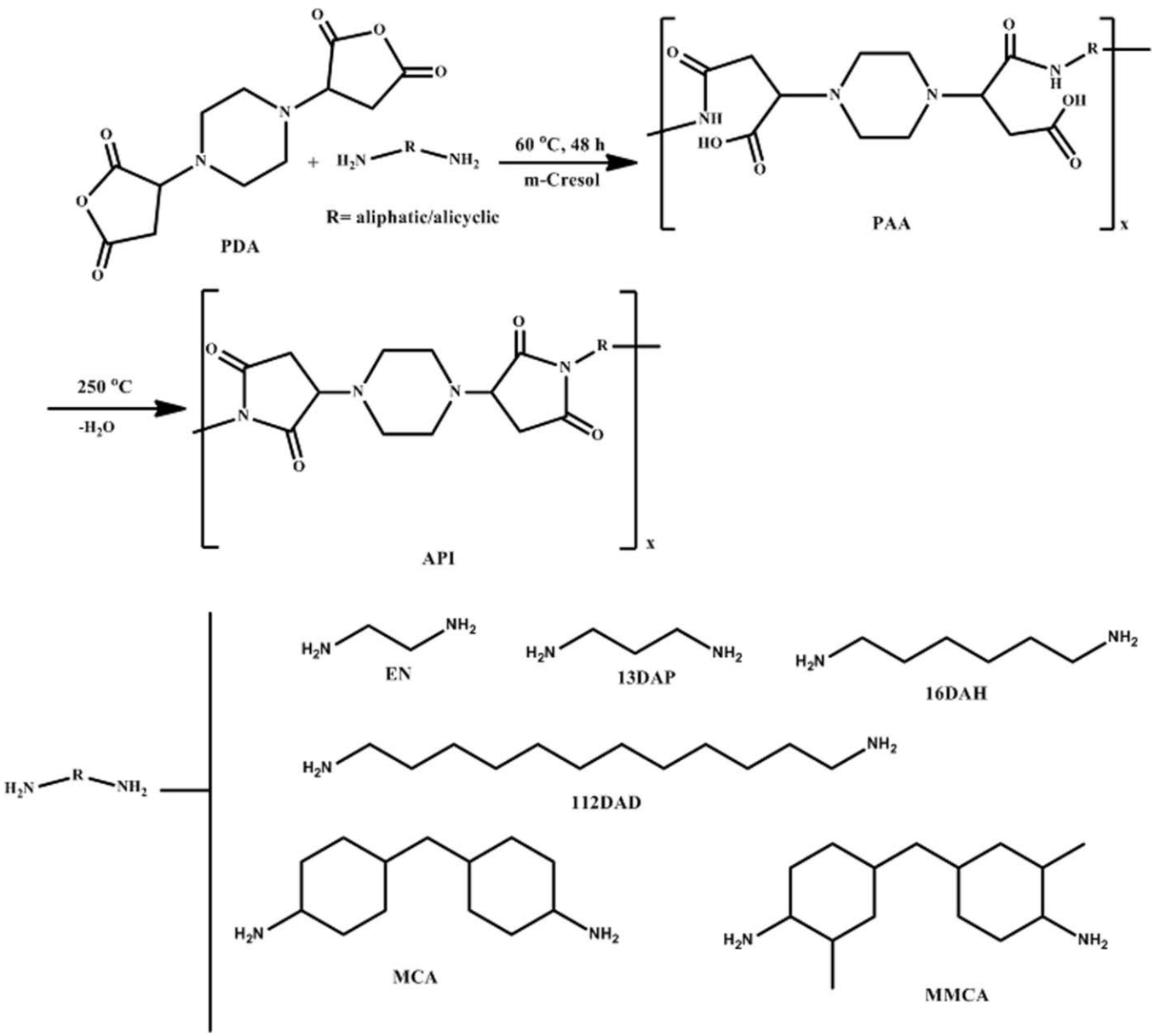

SCHEME 2 Synthesis of aliphatic polyimides.

which support unambiguously the structure shown in Scheme 1. The analytical data of PDA and the intermediate compounds DMF, PDSTE, and PDSTA were given in the experimental section (scanned spectra are provided in the Supporting Information). The results indicate the successful synthesis of novel piperazine containing dianhydride monomer (PDA) in this work.

Polyimides Synthesis and Characterization

For the synthesis of APIs, six different aliphatic diamines were used (Scheme 2). Ethylene diamine (EN), 1,3-diaminopropane (13DAP), 1,6-diaminohexane (16DAH), and 1,12-diaminododecane (112DAD) were selected as flexible linear aliphatic diamines with the intention of studying the impact that increasing chain length and flexibility has upon the inherent characteristics of the APIs. Two alicyclic monomers 4,4′-methylene bis(cyclohexylamine) (MCA), and 4,4′-methylene bis(2-methylcyclohexylamine) (MMCA) were selected with the objective to study how the basic traits of the polyimides vary with respect to the effects of the methyl substituent, and steric hindrance of their diamine subunits.

The APIs were prepared by a conventional two-step procedure through a ring-opening polyaddition to give PAAs and the subsequent thermal imidization (Scheme 2) at higher temperature. Carboxylic acid salts generally result from the reactions of dianhydrides with highly basic diamines, such as aliphatic and alicyclic diamines, together with polyamic acids. This salt formation prevents the isolation of high molecular-weight polyamic acids. Salt formation can be reduced considerably by using higher reaction temperature (~60 °C) for

TABLE 1 Elemental Analysis and GPC Molar Mass of APIs

Diamine	Polyimide Code		Elemental Analysis (%) C	H	N	GPC Molar Mass 10^4 M_n	PDI
16DAH	API3	Calcd.	59.49	7.49	15.42	2.19	1.6
		Found	58.79	7.02	15.58		
112DAD	API4	Calcd.	64.40	8.78	12.52	2.23	1.8
		Found	63.72	8.27	13.04		
MCA	API5	Calcd.	65.62	8.15	12.24	3.2	2.3
		Found	64.51	7.92	12.01		
MMCA	API6	Calcd.	66.78	8.51	11.54	2.9	2.3
		Found	66.02	8.62	10.95		

PAA preparation. Therefore, we prepared our APIs by two step procedure: first formation of PAAs at 60 °C in *m*-cresol and then thermal imidization of the PAAs under programmed curing temperatures. The reaction of PDA with most basic amines, namely, EN and 13DAP, yielded lower molecular weight (M_n) (3800 and 4700) polyimides (Supporting Information Table S1) while relatively higher molecular weights (32,000 and 29,000) were resulted when alicyclic diamines (MCA and MMCA) were used (Table 1). Extensive salt formation by more basic EN and 13DAP prevents the formation of high molecular weight PAAs which led to the isolation of APIs with lower molecular weights. PDI of these APIs was in the range 1.6–2.3. Nevertheless, these results demonstrate that the dianhydride monomer PDA has good polymerization activity for forming APIs. Table 1 summarizes the GPC results of these APIs.

The chemical structures of APIs were confirmed by ^{1}H NMR and FTIR spectroscopy and by Elemental Analysis. In Figure 3, a typical ^{1}H NMR spectrum of the API4 is reported in which all the peaks were clearly assigned: the down field protons are of PDA while two most up field peaks can be attributed to the protons of 112 DAD. The protons of PDA residue appear at 3.82 ppm [-CH_2, 2,2'], 3.33 ppm [-CH_2CO, 1,1'], 2.74 ppm [-NCH_2, 3] and 2.40 ppm [-NCH_2, 4] while that of 112 DAD at 1.44 ppm [-NCH_2, 5] and at 1.22 ppm [-CH_2, 6]. The absence of any peaks above 10 ppm (10–14 ppm) confirms complete imidization.

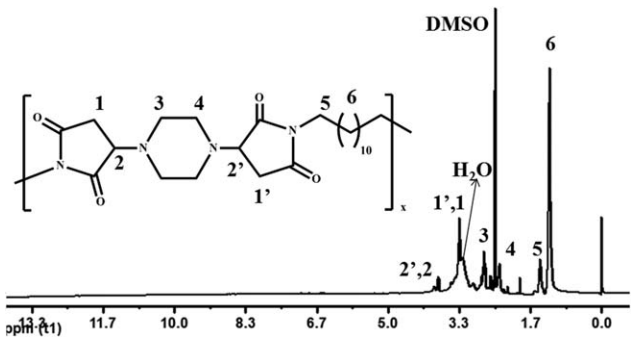

FIGURE 3 ^{1}H NMR spectrum of API4 in d_6-DMSO.

In the FTIR spectra (Fig. 4) of all the polyimides showed characteristic imide absorption bands at 1771–1775 cm^{-1}, which were attributed to the asymmetrical carbonyl stretching vibrations, and at 1691–1697 cm^{-1}, which were attributed to the symmetrical carbonyl stretching vibrations. Nonconjugations of the imide carbonyl group due to the absence of an aromatic ring cause the absorption shift in the APIs. Apart from these two carbonyl stretching frequencies, additional peaks at 1625 and at 1622 cm^{-1} appeared in case of API1 and API2, respectively. This may be interpreted as the C=O stretching of amide of their polyamic acids (PAA). Salt formation by these two extremely basic diamines (EN and DAP) with PDA prevents them from complete imidization. Incomplete imidization of these two diamines can also be understood from the appearance of relatively broader IR peaks centred around 3400 cm^{-1} (O-H and N-H stretching frequencies of PAA) in the FTIR spectra of API1 and API2. In case of the remaining four APIs, there were no characteristic absorption bands of the amide group around

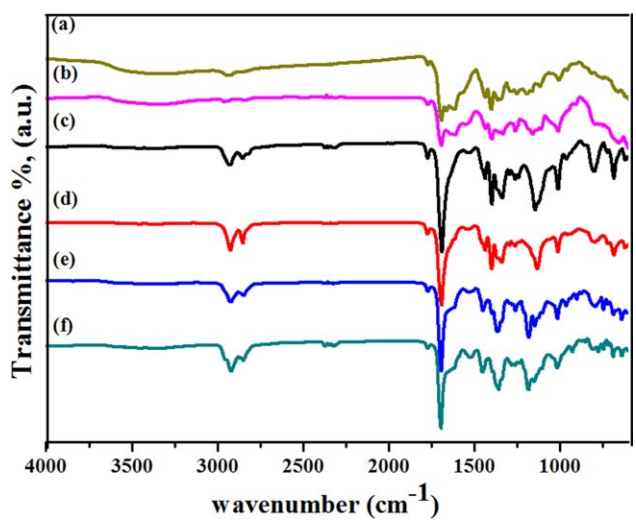

FIGURE 4 FTIR spectra of the aliphatic polyimides: (a) API1, (b) API2, (c) API3, (d) API4, (e) API5, and (f) API6. [Color figure can be viewed in the online issue, which is available at wileyonlinelibrary.com.]

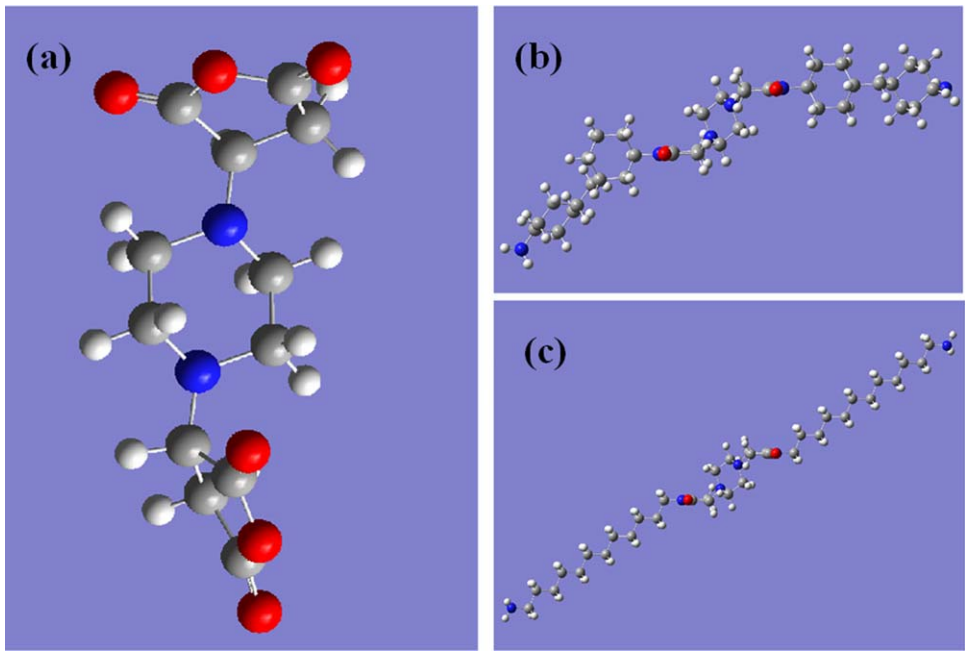

FIGURE 5 Molecular structures of (a) PDA; (b) API4; (c) API5. Gray, white, red, and blue each molecular structure display C, H, O, and N, respectively. The geometries were optimized by the DFT (B3LYP/6–311G(d,p)) calculations. [Color figure can be viewed in the online issue, which is available at wileyonlinelibrary.com.]

3300 cm^{-1} (O-H and N-H stretching frequencies of PAA) or 1630–1640 cm^{-1} (C=O stretching), indicating that the polymers had been fully imidized. In all cases, we observed peaks at around 1360 cm^{-1} due to the C-N stretching. Because of the presence of so many different types of C-N bonds in the API backbone, however, it was rather difficult to assign them all. The elemental analysis values of the polymers generally agreed well with the calculated values for the proposed structures. The results of the elemental analyses of the polyimides are listed in Table 1 and Supporting Information Table S1. The observed values were in good agreement with the calculated ones.

Molecular Structures

Figure 5 shows the three-dimensional molecular structures of PDA and its two representative polyimides (API4 and API5). The geometries were optimized by the DFT calculations using a large basis-set function.[26–31] From the optimized structure, it is revealed that PDA has (R,S) configuration at the two stereo centers present in it. The two dianhydride units are not completely trans (parallel) to each other. The two planes containing the two dianhydride units make an angle of 94°, which means that they are almost perpendicular. On the other hand, in API4 and API5, two dianhydride planes (now imide plane) are almost parallel (dihedral angle is 179°). Therefore, after imidization, the strain in the polymer chain forced these planes to be nearly parallel in order to avoid the steric repulsion.

It is very interesting to observe that even though the imide planes are parallel in both API4 and API5, the polyimide chain in API4 is almost linear while in API5 is nonlinear and to some extent distorted as well. API4 contain long, linear, alkyl chain diamine (1,12-diaminododecane) which can arrange in a zigzag fashion to give it a linear shape while the presence of rigid, bulky alicyclic diamine (MCA) ensure it to be distorted and nonlinear in shape. These subtle changes in the chain geometry of these two kinds of polyimides, resulted in enormous differences in their properties as we are going to witness in the following discussions. The nonlinear, distorted conformation of the polyimide chains in API5 and API6, effectively reduces the interchain charge transfer interaction and creates free-space in the polyimide matrix and thereby increases the solubility and decreases the color of these polyimides significantly.

Solubility

The solubility of the synthesized APIs was investigated in different organic solvents. All the APIs showed excellent solubility in *m*-cresol and in H_2SO_4. Apart from API1 and API2, other APIs exhibited complete solubility in polar solvents like NMP, DMAc, DMF, and DMSO only upon heating at 60 °C. Now this is quite interesting, because the presence of flexible aliphatic and alicyclic-backbone in the APIs should have resulted in APIs with higher solubility in both polar and nonpolar solvents. The relatively moderate solubility of these APIs may be due to the presence of the nucleophilic (electron-donating) aminomethylene group (-NCH_2) in the piperazine unit of the dianhydride segment of the APIs which could have electrostatic interaction with electrophilic (electron-withdrawing) carbonyl groups in imide and thereby strengthen the intermolecular interactions that are used to be very less in so called APIs. Polyimides resulted from EN and 1,3-diaminopropane were quite soluble in water which

TABLE 2 Solubility Data of the Polyimides Synthesized in This Work

	Solvents[a]								
API	NMP	DMAc	DMF	DMSO	*m*-Cresol	$CHCl_3$	H_2O	Pyridine	H_2SO_4
API3	+	+	+	+	++	–	±	+	++
API4	+	+	+	+	++	–	±	+	++
API5	+	+	+	+	++	–	–	+	++
API6	+	+	+	+	++	–	–	+	++

[a] Solubility: (++) soluble at room temperature; (+) soluble upon heating at 60 °C; (±) partially soluble or swells; (–) insoluble.

may be due to the extensive salt formation by these relatively basic diamines with PDA. The solubility behavior of these polymers in different solvents is presented in Table 2 and Supporting Information Table S2.

Optical Properties

Fully APIs normally exhibit high transparency because of their low molecular density, polarity, and probabilities of mediating inter- and intramolecular CT. Figure 6 shows the UV–visible absorption spectra of the polyimide films with a thickness of 15 μm. Three distinct types of polyimides were obtained after the thermal imidization of the polyamic acid solutions of PDA with six different diamines. The polyimide films of EN and 13DAP with PDA were highly brittle and reddish-black in color while flexible, free-standing yellow colored films were obtained with 16-DAH and 112-DAD. But, by far, the most transparent polyimide films (API5 and API6) were obtained by alicyclic diamines (MCA and MMCA). These films were almost colorless with a very little yellowish tint. As shown in Figure 6, all the polyimides showed a shoulder absorption band at higher wavelength region in addition to the main absorption band that occurred at the shorter wavelength region. The absorption edges (λ_E) of these two absorption band of each polyimide film were estimated by the point where the absorption curve intersects a bisected line drawn through the intersection of the extrapolations of the two slopes. The absorption edges (λ_E) for API3, API4, API5, and API6 were 369, 349, 339, and 333 nm, respectively, while the same for shoulder absorption band were 454, 447, 429, and 427 nm, respectively. Because of the tailing of these shoulder absorption bands in the visible region, none of these polyimide films were completely colorless. The shoulder absorption bands of API5 and API6 (with MCA and MMCA) were less intense and also appeared at shorter wavelengths. Hence, these polyimide films were very less colored. The occurrences of the shoulder absorption bands in addition to main absorption bands certainly indicate that there may be two energy band gaps: lower energy band gap may be from dianhydride while the higher energy band gap from diamines.

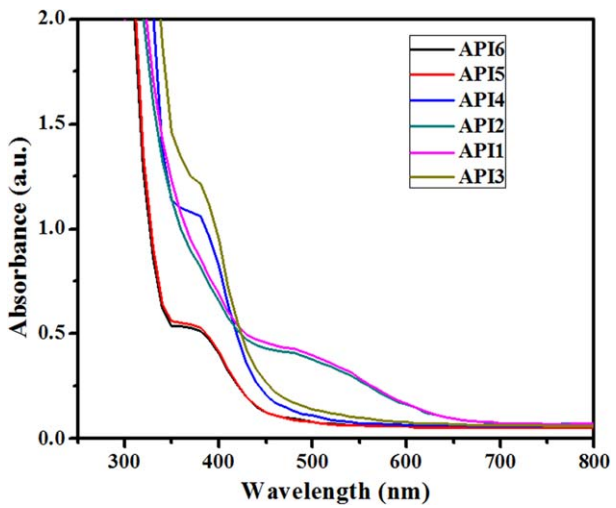

FIGURE 6 UV–visible absorption spectra of API films. [Color figure can be viewed in the online issue, which is available at wileyonlinelibrary.com.]

Figure 7 shows the optical transmission spectra of the API films. The spectra are principally the same as those shown in Figure 6. However, it is important to understand the difference in the optical transparency at the longer wavelengths. As expected, APIs with alicyclic diamines (API5 and API6) exhibited highest transmittance of 88% above 450 nm wavelength region while APIs with longer linear aliphatic diamines (API3 and API4) showed around 86%

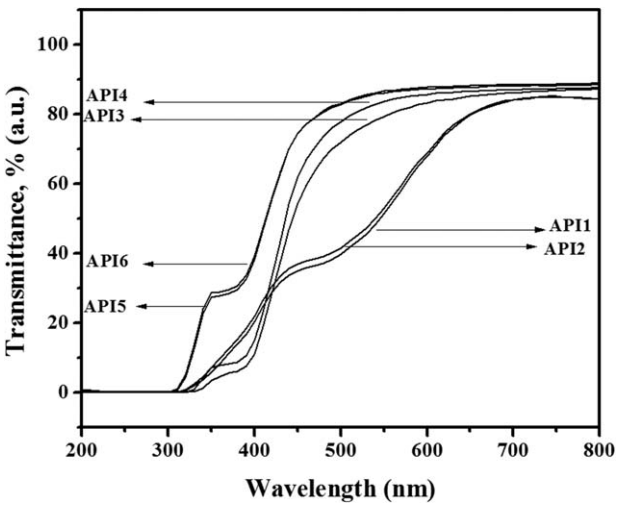

FIGURE 7 Optical transmission spectra of API films.

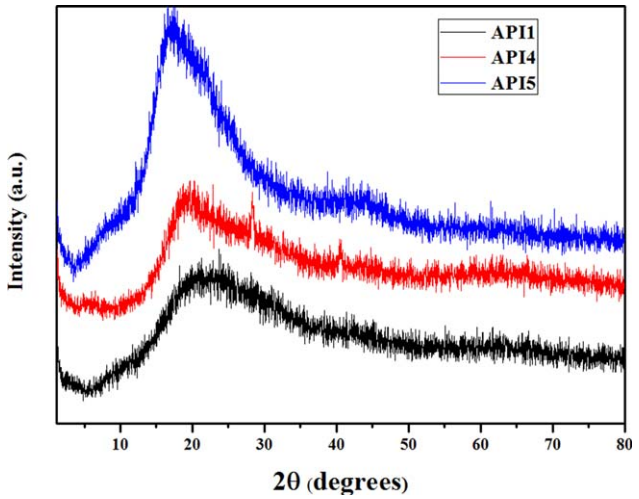

FIGURE 8 XRD patterns of APIs. [Color figure can be viewed in the online issue, which is available at wileyonlinelibrary.com.]

transmittance above 500 nm. APIs with short linear aliphatic diamines (EN and 13-DAP) exhibited lowest transmittance. These films were reddish-black in color. Linear APIs have more densely packed chain structures compared to APIs with bulky, nonlinear alicyclic diamines (MCA and MMCA). Again, APIs with linear, short alkyl chain diamines (EN and 13-DAP) possess higher density of electrophilic amide group and nucleophilic aminomethylene groups (-NCH_2). These two factors lead to the considerable degree of interchain charge transfer interaction in the linear alkyl chain polyimides and API1 and API2 with very short alkyl chain diamines experienced maximum CT interaction leading to highly colored polyimide films much like aromatic polyimides. APIs with bulky and nonlinear alicyclic diamines effectively reduce the interchain CT interaction and thereby yielded almost colorless polyimide films. The extreme broadening of the optical transmission spectra of API1 and API2 is also an indication of the existence of severe charge transfer interaction between the polymer chains.

Crystallinity

Figure 8 shows WAXD patterns of three representative APIs (API1, API4, and API5). For all these three polyimides, the reflection patterns are featureless, showing only broad amorphous halos that appeared in the region $2\theta = 5–38^\circ$ and centered around $2\theta = 20^\circ$. This is due to the diffraction of a poor intermolecular packing combined with amorphous halo.[32] The broad peaks gradually shifted toward higher 2θ values as we moved from alicyclic diamine to short chain aliphatic diamine through long chain aliphatic diamine-based polyimides (API5, $2\theta = 17.2^\circ$, d-space = 5.2 Å; API4, $2\theta = 19.4^\circ$, d-space = 4.6 Å; API1, $2\theta = 21.8^\circ$, d-space = 4.1 Å). The d-spacing is usually considered to represent the distance between segments of different chains and related to the free volume of a polymer. Introduction of the bulky, nonlinear alicyclic moieties in the polymer backbone may be to some extent contributed to the disruption of the internal order of the polymer chains in the alicyclic diamine-based API5 which registered highest d-spacing. In API1, because of the presence of short alkyl chain diamine, the internal order in the polymer matrix is very high which is revealed from its lower d spacing value (4.1 Å). Now as the chain length of the aliphatic diamine part increases (API4), the flexibility of the polyimides also increases and that to some extent disrupts the internal order of the polymer chains and eventually leads to the polyimide (API4) with higher d-spacing than that of short alkyl chain aliphatic diamine-based polyimide (API1). Normally, as the d-spacing value increases, the free volume also increases and so as the solubility of polymer.[33] API5 with higher d-spacing value showed higher solubility in common organic solvents than API1 with lower d-spacing value.

Mechanical and Dielectric Properties

The mechanical properties of the fully APIs (API6, API5 and API3, and API4) were investigated using the stress–strain curves (Fig. 9) obtained from UTM and the average values of five different measurements for each APIs are listed in Table 3. All these four polyimides showed appreciable mechanical stiffness, tensile strength varying from 54 to 72 MPa, elongation at break from 4 to 9%, and tensile modulus in the range 1.6–2.3 GPa (Table 3). API4 and API3 with flexible, linear, long alkyl chain aliphatic diamines exhibited the lowest tensile strength and highest percentage of elongation at break while API6 and API5 with more rigid, bulky alicyclic diamines, demonstrated highest tensile strength and lowest percentage of elongation at break. Usually, the linear aliphatic polymers have low rigidity and tensile strength because of the flexible and compliant chain structures, thus these enhanced mechanical strength may be due to appreciable charge transfer interaction between the nucleophilic (electron donating) aminomethylene group (-NCH_2) in the piperazine unit of the dianhydride and electrophilic (electron withdrawing) carbonyl groups in imide. The polyimide films of API1 and API2 were too brittle to measure their mechanical properties by UTM.

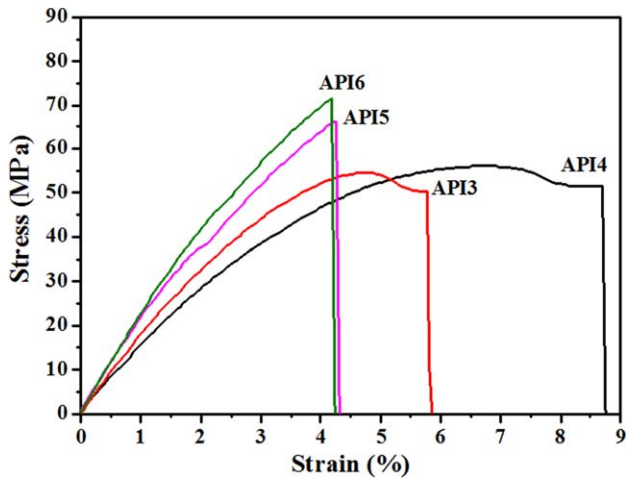

FIGURE 9 Stress–strain curves of APIs. [Color figure can be viewed in the online issue, which is available at wileyonlinelibrary.com.]

TABLE 3 Thermal, Mechanical Properties, and Dielectric Constants of API Films

APIs	Tensile Strength (Mpa)	Elongation at Break (%)	Tensile Modulus (Gpa)	Dielectric Constant (ε)	λ_{ex} (nm)	λ_{ex} (nm)	T_d^5 (°C)	T_d^{10} (°C)	T_g (°C)[a]	T_g (°C)[b]
API3	55±8	6±1	1.8±0.2	2.67	355	505	323	360	212	196
API4	54±7	9±1	1.6±0.2	2.14	364	498	286	307	170	172
API5	66±10	4±1	2.1±0.5	3.30	381	488	382	418	224	218
API6	72±9	4±1	2.3±0.4	2.87	386	491	376	413	237	233

[a] Measured by DSC.

[b] Peak temperature of tan(δ) in the DMA thermogram.

The dielectric constant (ε) was varied according to the type of diamine monomers used: the lowest value was measured for API4 ($\varepsilon = 2.14$) (Table 3), whereas the highest value was obtained for API2 ($\varepsilon = 5.09$) (Supporting Information Table S3).

The lowest dielectric constant of API4 (with 112DAD) is considered due to the long alkyl chain that reduces the number of polarizable molecular units in a given volume. Generally, APIs possessed low dielectric constant due to the diminution in the degrees of chain packing and interchain interactions.[34] The dielectric constant of API4 was even lower than polyethylene (extensively used in various dielectric applications). Polyethylene (plastic) is a tough inexpensive polymer made of long chains of carbons attached with hydrogens. It has fine dielectric properties with its low dielectric constant (2.3) and low moisture absorption; however, as the temperature increases, it tends to soften as its crystallites melt and its dielectric strength will decrease. As we move on to end of this discussion, we will find that API4 is thermally much more stable (T_d^5 286 °C and T_g 170 °C) than polyethylene (T_g of low-density polyethylene is −120 °C, while melting temperature (T_m) is 135 °C) and this make API4, a very promising materials for high temperature dielectric applications. The abnormally high dielectric constant of API1 and API2 (Supporting Information Table S3) may be due to the presence of extensive interchain CT interaction between the nucleophilic (electron donating) aminomethylene group (-NCH_2) in the piperazine unit of the dianhydride and electrophilic (electron withdrawing) carbonyl groups in the imide. The increased density of polar imide groups in these two APIs may also contributed to their much enhanced dielectric constant values. APIs with alicyclic diamines (API5 and API6) showed higher dielectric constants than expected as the presence of the highly rigid and bulky alicyclic moieties, which sterically hinder the packing and enlarge the free volume in the polyimides, inducing low dielectric properties.[35] Interchain CT interactions might have contributed to some extent in these cases as well.

Fluorescent Properties

Fluorescent spectroscopy is used widely to examine the electronic structures and aggregation states of polymers on account of its high sensitivity to microenvironmental changes in polymer matrices.[36] Figure 10 shows the one-dimensional excitation and emission spectra of the API films. All API films showed an apparent fluorescent emission in the visible region. Table 3 lists the wavelengths of the excitation and emission peaks. The Stokes shifts were estimated from the difference in wavelength between the excitation and emission peaks. The API5 and API6 based on alicyclic diamines (MCA and MMCA) show excitation peaks at 381and 386 nm and emission peaks at 488 and 491 nm, and the calculated Stokes shifts were 0.71 and 0.69 eV, respectively. The API3 and API4 based on long aliphatic chain diamines (16DAH and 112DAD) show excitation peaks at 355 and 364 nm and emission peaks at 505 and 498 nm, and the calculated Stokes shifts were 1.04 and 0.92 eV, respectively.

The Stokes shifts of API3 and API4 are much larger than that of the API5 and API6. The large Stokes shifts values in API3 and API4 and along with their relatively broaden nature of fluorescent emission spectra clearly indicate the existence of significant CT interactions in the polyimide network that is quite typical with aromatic polyimides.[37] These CT interactions are weakened considerably in API5 and API6 due to the presence of bulky and rigid alicyclic diamines. The excitation and emission spectra of API2 are too broad to measure the corresponding λ_{max} values. This extreme broad nature of the fluorescent emission spectra once again demonstrates the existence of enormous CT interaction in API2 originating from the very high density of nucleophilic (electron donating) aminomethylene group (-NCH_2) in the piperazine unit of the dianhydride and electrophilic (electron withdrawing) carbonyl groups in imide.

Thermal Stability and Phase Transitions

The thermal properties of all APIs were evaluated by TGA, DSC, and DMA measurements. Figure 11 displays representative TGA curves; Table 3 and Supporting Information Table S3 summarize the results. The polymers underwent their 5% weight losses within the temperature range from 286 to 382 °C. The temperatures for 10% gravimetric loss (T_{10}), which is an important criterion for evaluating thermal stability, were in the range 299–418 °C. The polyimides containing linear aliphatic chains on their backbones were the least resistant to temperature. It already has been reported that the thermal stability of aliphatic linear diamine-based polyimides decreased upon increasing the length of their thermally fragile alkyl chains (mainly because of the dilution

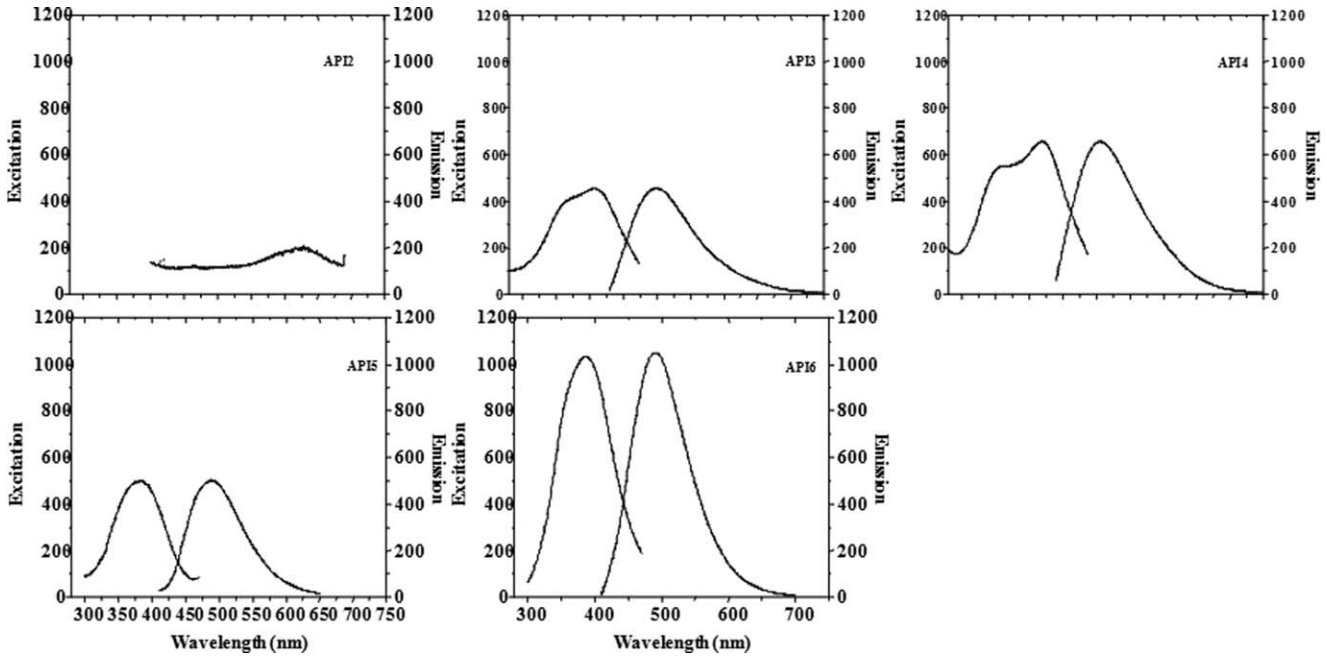

FIGURE 10 Excitation and fluorescent emission spectra of APIs.

effect of aliphatic imide moieties).[9] The synthesized APIs with linear alkyl chain exhibited some confusing results. API1 and API4 with shortest and longest alkyl chain show the lowest T_d[5] (286 °C). API3 with longer alkyl chain was more stable than short alkyl chain API2. On the other hand, as predicted earlier, API3 with six carbon alkyl chain diamine was thermally more stable than its 12 carbon counterpart API4. This apparently anomalous behavior of API1 and API2 may be due to their incomplete imidization that left considerable number of thermally labile amic acid groups in the polymer backbone and thereby result polyimides with lower thermal stability. API2 was thermally more stable than API1 due to its higher degree of imidization as evident from their FTIR spectra (Fig. 4). The thermal stability of the APIs was improved significantly when aliphatic diamines were replaced by alicyclic diamines (MCA and MMCA). API5 and API6 with rigid alicyclic diamines were found to be stable even up to 400 °C (T_d[10] 418 and 413 °C, respectively). Apart from the rigid nature of these two alicyclic diamines, the charge transfer interaction in API5 and API6 (as is evident from large Stokes shifts in the excitation and fluorescent emission spectra) may have played a crucial role in improving the thermal stability of these two polyimides. The residual weight of API1 and API2 were 30 and 33% at 800 °C that are much higher than the rest of the polyimides. The densities of the thermally stable imide units in API1 and API2 (with short alkyl chain diamines) are higher than the remaining polyimides and this may have contributed to the higher residual weight of API1 and API2 at 800 °C.

The glass transition temperatures (T_g) of APIs were determined by DSC (Fig. 12) and DMA (Fig. 13). No significant changes were observed in the DSC analysis of API1 and API2 up to 300 °C. The glass transition temperatures (T_g) of API3-API6 were in the range of 170–237 °C. The results are summarized in Table 3. For, pure APIs (API3 and API4), the glass transition temperatures decreased with increasing the aliphatic chain length of the diamines. The greater flexibility of 1,12-diaminododecane in API4 brought down its T_g to 170 °C in comparison to 1,6-diaminohexane in API3 which showed the glass transition at 212 °C. Polyimides with alicyclic diamines (API5 and API6) showed higher T_g in comparison to the polyimides with linear aliphatic diamines (API3 and API4). The increased chain rigidity due to the incorporation of rigid alicyclic diamines restricted the free rotation about the polymer and hence produced polyimides with higher T_g values. The enhanced values of T_g of API6

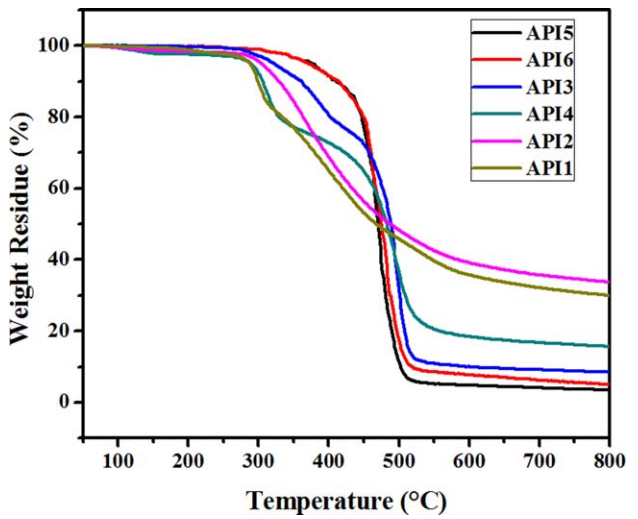

FIGURE 11 TGA curves of the APIs. [Color figure can be viewed in the online issue, which is available at wileyonlinelibrary.com.]

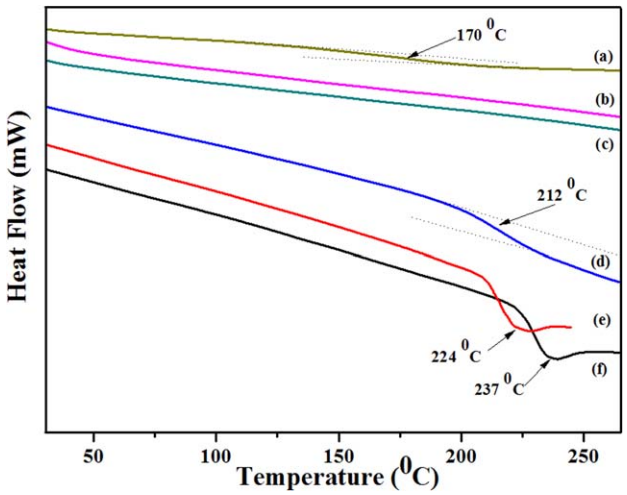

FIGURE 12 DSC thermograms of the APIs: (a) API4; (b) API1; (c) API2; (d) API3; (e) API5 and (f) API6. [Color figure can be viewed in the online issue, which is available at wileyonlinelibrary.com.]

possessing MMCA backbones, relative to those possessing MCA units, suggest that the glass transition temperatures of these types of polyimides increase gradually upon increasing the chain rigidity induced by the methyl substitution. Figure 13 shows the variations in the storage modulus (E') and loss factor (tan δ) at different temperatures. The thermograms show the α-relaxation (main peaks) between 160 and 250 °C. In the DMA thermograms, the T_g was estimated from the peak temperature of tan δ curve. The T_gs for API3, API4, API5, and API6 were observed at 196, 172, 218, and 233 °C, respectively. The glass transitions were increased considerably by replacing long chain aliphatic diamines (16DAH and 112DAD) with comparatively rigid alicyclic diamines (MCA and MMCA). The T_gs estimated from DSC and DMA were almost similar except API3. The estimated T_g of API3 by DMA was substantially lower than that obtained by DSC. The DSC curve of API3 was in fact too flat (Fig. 12) to estimate

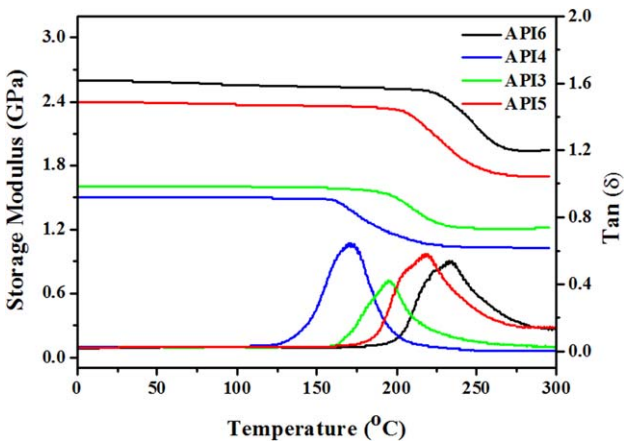

FIGURE 13 Temperature dependence of storage modulus and tan δ for APIs. [Color figure can be viewed in the online issue, which is available at wileyonlinelibrary.com.]

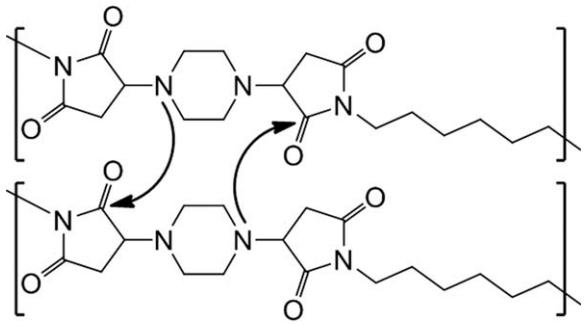

FIGURE 14 The intermolecular charge transfer/electrostatic interaction in APIs of PDA.

the infletion point accurately. It can be seen from Figure 13 that the storage modulus of APIs remains almost constant on heating below their glass transition temperatures. The storage modulus at room temperature of API3, API4, API5, and API6 were 1.6, 1.5, 2.4, and 2.6 GPa, respectively, which were comparable to their tensile modulus estimated from the stress–strain curves (Fig. 9) obtained from UTM. API5 and API6 with rigid alicyclic diamines exhibited higher storage modulus than flexible, long alkyl chained APIs (API3 and API4). Unfortunately, the polymer films of API1 and API2 were too brittle to analyze by DMA.

Presence of electron withdrawing groups in the dianhydride structure and electron donating groups in the diamine structure lead to strong charge transfer complex (CTC) formation which consequently results more colored polyimides.[38,39] The lack of color in aliphatic and alicyclic polyimides is due to the absence or inhibition of intra and/or intermolecular charge-transfer interactions. On the other hand, in case of PDA, the nucleophilic (electron-giving) trimethyleneamino group can have electrostatic/intermolecular charge transfer interaction with electrophilic (electron-withdrawing) carbonyl groups in imide (Fig. 14), although the N atoms in imide groups also have lone electron pairs, they are delocalized by the resonance of electron-withdrawing carbonyl groups next to it and are unavailable for such kind of interaction. This kind of interchain interaction is different from the so-called charge transfer interaction in aromatic polyimides where the major part of polymer chain is in conjugation. Since the nucleophilic trimethyleneamino group in PDA is not in conjugation with the electrophilic carbonyl group, it has a very little influence on the electron accepting property (electron affinity) of the carbonyl group. The absence of conjugation in PDA inhibits all kinds of possible intramolecular charge transfer interactions (interactions are mainly through space not through bonds). Intermolecular charge transfer/electrostatic interactions between electron giving trimethyleneamino groups and electron-accepting carbonyl groups are the only possible interactions between the polymer chains of APIs of PDA and this kind of interchain interactions in PDA containing APIs were mainly responsible for their higher thermal mechanical stabilities and lower transparencies than the traditional aliphatic/alicyclic polyimides.

CONCLUSIONS

Six new fully APIs based on a novel aliphatic dianhydride monomer-2,2′-(1,4-piperazinediyl)-disuccinic anhydride (PDA), in which two units of succinic anhydride have been connected by an aliphatic heterocyclic piperazine spacer that possesses aminomethylene (-NCH_2) moiety in the aliphatic/alicylic backbone capable of inducing charge transfer (CT) interactions in the polyimide network, were successfully synthesized by a two-step polycondensation method using four aliphatic and two alicyclc diamines. The polyimides (API3-API6) produced organo-soluble, free-standing, less-colored films with reasonable thermal, mechanical properties. T_{10} (temperature of 10% weight loss) of APIs were ranged from 299 to 418 °C, T_g of API3-API6 were in the temperature range of 170–237 °C, tensile strength of 54–72 Mpa, tensile modulus of 1.6–2.3 Gpa, and elongation at break of 4–9%. The dielectric constant of one of the synthesized API (API4) was as low as 2.14. This thermally stable ultra-low dielectric polyimide could be a very promising material for high-temperature dielectric applications. Charge transfer/electrostatic interaction in APIs induced by nucleophilic aminomethylene group (-NCH_2) was mainly responsible for showing intermediate behavior (between aliphatic and aromatic polyimides) by these APIs.

ACKNOWLEDGMENTS

The work was supported by the National Research Foundation of Korea (NRF). Grant funded by the Ministry of Science, ICT, Future planning, Korea (Acceleration Research Program (No. 2009-0078791); Pioneer Research Center Program (No. 2010-0019308/2010-0019482); and the Brain Korea 21 Plus Program(21A2013800002)).

REFERENCES AND NOTES

1 Polyimides Fundamentals and Applications; M. K. Ghosh, K. L. Mittal, Eds.; Marcel Decker: New York, **1996**.

2 D.-J. Liaw, K.-L. Wang, Y.-C. Huang, K.-R. Lee, J.-Y. Lai C.-S. Ha, *Prog. Polym. Sci.* **2012**, *37*, 907–974.

3 S. Tamai, H. Oikawa, M. Ohta, A. Yamaguchi, *Polymer* **1998**, *39*, 1945–1949.

4 I. K. Spiliopoulos, J. A. Mikroyannidis, *Macromolecules* **1998**, *31*, 522–529.

5 Y. Kim, J.-H. Chang, *Macromol. Res.* **2013**, *21*, 228–233.

6 H. Seino, T. Sasaki, A. Mochizuki, M. Ueda, *High Perform. Polym.* **1999**, *11*, 255–262.

7 X. Z. Jin, H. Ishii, S. Segawa, *J. Photopolym. Sci. Technol.* **2005**, *18*, 313–318.

8 E. Y. Chung, S. M. Choi, H. B. Sim, K. K. Kim, D. S. Kim, K. J. Kim, M. H. Yi. *Polym. Adv. Technol.* **2005**, *16*, 19–23.

9 A. S. Mathews, I. Kim, C.-S. Ha, *J. Appl. Polym. Sci.* **2006**, *102*, 3316–3326.

10 H.-C. Yu, S. V. Kumar, Y.-K. Song, J. Choi, K. Kudo, J.-G. Kim, S.-Y. Oh, C.-M. Chung, *Macromol. Res.* **2011**, *19*, 1272–1277.

11 D.-J. Liaw, B.-Y. Liaw, *Macromol. Chem. Phys.* **1999**, *200*, 1326–1332.

12 D.-J. Liaw, B.-Y. Liaw, C.-Y. Chung, *Macromol. Chem. Phys.* **1999**, *200*, 1023–1027.

13 D.-J. Liaw, B.-Y. Liaw, *Polym. J.* **1999**, *31*, 1270–1273.

14 D.-J. Liaw, C. C. Huang, W. H. Chen. *Macromol. Chem. Phys.* **2006**, *207*, 434–443.

15 G. O. Schenck, W. Hartmann, S. P. Mannsfeld, W. Metzner, C. H. Krauch. *Chem. Ber.* **1962**, *95*, 1642–1647.

16 H. Suzuki, T. Abe, K. Takaishi, M. Narita, F. Hamada, *J. Polym. Sci. Part A: Polym. Chem.* **2000**, *38*, 108–116.

17 T. Matsumoto, *Yuki Gosei Kagaku Kyokaishi* **2000**, *58*, 776–786.

18 M. I. Fremery, E. K. Fields, *J. Org. Chem.* **1963**, *28*, 2537–2541.

19 A. Maggiolo, A. L. Tumolo, U.S. Patent 3023233, **1962**.

20 G. W. Smith, H. D. Williams, *J. Org. Chem.* **1961**, *26*, 2207–2212.

21 Y. T. Chern, W. H. Chung, *J. Polym. Sci. Part A: Polym. Chem.* **1996**, *34*, 117–124.

22 W. Volksen, H. J. Cha, M. I. Sanchez, D. Y. Yoon, *React. Funct. Polym.* **1996**, *30*, 61–69.

23 B. Li, T. Liu, W.-H. Zhong, *Polymer* **2011**, *52*, 5186–5192.

24 G. Carr, D. E. Williams, A. R. Díaz-Marrero, B. O. Patrick, H. Bottriell, A. D. Balgi, E. Donohue, M. Roberge, R. J. Andersen, *J. Nat. Prod.* **2010**, *73*, 422–427.

25 T. Makoto, Y. Kazuhiro, D. Matsumi, W. Masaaki, M. Hiroyuki, K. Toshimitsu, Y. Naohisa, K. Yoshitane, *Bull. Chem. Soc. Jpn.* **2001**, *74*, 707–715.

26 S. Ando, T. Fujigawa, M. Ueda, *Jpn. J. Appl. Phys.* **2002**, *41*, L105.

27 Gaussian 03, Revision D.02; Gaussian, Inc.: Wallingford, CT, **2004**.

28 G. Slonimskii, A. Askadskii, A. Kitaigodorodskii, *Polym. Sci. USSR* **1970**, *A12*, 556.

29 A. Bondi, *J. Phys. Chem.* **1964**, *68*, 441.

30 S. Ando, *J. Photopolym. Sci. Technol.* **2006**, *19*, 351.

31 Y. Terui, S. Ando, *J. Photopolym. Sci. Technol.* **2005**, *18*, 337.

32 N. Takahasi, D. Y. Yoon, W. Parrish, *Macromolecules* **1984**, *17*, 2583–2588.

33 L. Xiong, X. Wang, H. Qi, F. Liu, *J. Appl. Polym. Sci.* **2013**, *127*, 1493–1501.

34 Y. T. Chern, H. C. Shiue, *Macromol. Chem. Phys.* **1998**, *199*, 963–969.

35 A. S. Mathews, I. Kim, C.-S. Ha, *J. Polym. Sci. Part A: Polym. Chem.* **2006**, *44*, 5254–5270.

36 M. Hasegawa, K. Horie, *Prog. Polym. Sci.* **2001**, *26*, 259–335.

37 M.-C. Choi, J. Wakita, C.-S. Ha, S. Ando, *Macromolecules* **2009**, *42*, 5112–5120.

38 R. A. Dinc-Hart, W. W. Wright, *Makromol. Chem.* **1971**, *143*, 189–192.

39 R. S. Mulliken, *J. Am. Chem. Soc.* **1952**, *74*, 811–824.